Inorganic Chemistry

ARTICLE

pubs.acs.org/IC

Hydrogen and Methanol Exchange Processes for (TMP)Rh-$OCH_3(CH_3OH)$ in Binary Solutions of Methanol and Benzene

Sounak Sarkar,[‡] Shan Li,[‡] and Bradford B. Wayland*[,†]

[†]Department of Chemistry, Temple University, Philadelphia, Pennsylvania 19122, United States

[‡]Department of Chemistry, University of Pennsylvania, Philadelphia, Pennsylvania 19104, United States

Supporting Information

ABSTRACT: Tetramesityl porphinato rhodium(III) methoxide ((TMP)Rh-OCH_3) binds with methanol in benzene to form a 1:1 methanol complex ((TMP)Rh-$OCH_3(CH_3OH)$) (**1**). Dynamic processes are observed to occur for the rhodium(III) methoxide methanol complex (**1**) that involve both hydrogen and methanol exchange. Hydrogen exchange between coordinated methanol and methoxide through methanol in solution results in an interchange of the environments for the non-equivalent porphyrin faces that contain methoxide and methanol ligands. Interchange of the environments of the coordinated methanol and methoxide sites in **1** produces interchange of the inequivalent mesityl *o*-CH_3 groups, but methanol ligand exchange occurs on one face of the porphyrin and the mesityl *o*-CH_3 groups remain inequivalent. Rate constants for dynamic processes are evaluated by full line shape analysis for the ^{1}H NMR of the mesityl *o*-CH_3 and high field methyl resonances of coordinated methanol and methoxide groups in **1**. The rate constant for interchange of the inequivalent porphyrin faces is associated with hydrogen exchange between **1** and methanol in solution and is observed to increase regularly with the increase in the mole fraction of methanol. The rate constant for methanol ligand exchange between **1** and the solution varies with the solution composition and fluctuates in a manner that parallels the change in the activation energy for methanol diffusion which is a consequence of solution non-ideality from hydrogen bonded clusters.

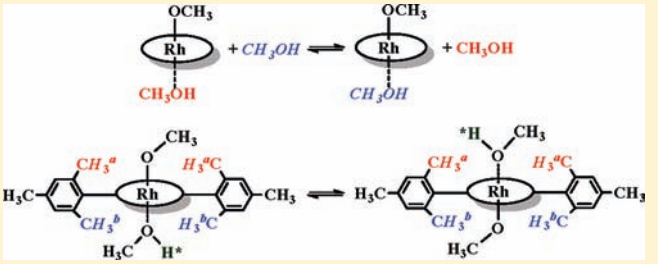

INTRODUCTION

Application of water and methanol as both solvent media and reactants is a current direction for organometallic catalysis research[1−15] and a central feature of our group nine metalloporphyrin reactivity and catalysis studies.[16−22] Water and methanol are high dielectric constant liquids[23,24] that have both hydrogen bonding and donor capability[25,26] which results in many similar features. Methanol is distinguished by having both hydroxylic and organic natures which result in the unusal property of miscibility in both water and organic hydrocarbon solvents. Miscibility of methanol and benzene permits varying the binary solution composition and properties continuously between the limits of the two pure liquids.[27−29] Reactivity studies of rhodium(III) tetramesityl porphyrin (TMP)Rh(III) complexes in binary solutions of methanol and benzene revealed dynamic processes involving coordinated methoxide and methanol of (TMP)Rh-$OCH_3(CH_3OH)$ (**1**)[30,31] (Supporting Information). This article reports on the effects of solution composition on exchange of hydrogen and methanol between **1** and binary solutions of methanol and benzene. The rate constant for interchange of the inequivalent porphyrin faces increases regularly with the increase in the mole fraction of methanol, but the rate of methanol ligand exchange shows unusual behavior by fluctuating as the solution composition changes. The rate costants for methanol ligand exchange from **1** vary with the solution composition in the same manner as the changes in the activation parameters for methanol diffusion in methanol/benzene solutions. This behavior is associated with non-ideality arising from the occurrence of hydrogen bonded clusters of methanol in methanol/benzene binary solutions.[32]

RESULTS AND DISCUSSION

Dissolution of the five-coordinate 16-electron rhodium(III) methoxide complex ((TMP)Rh-OCH_3) in methanol/benzene solvent media produces a solution of the six-coordinate 18-electron complex (TMP)Rh-$OCH_3(CH_3OH)$ (**1**)[30] (Supporting Information) (Figure 1).

Dynamic Processes Observed by ^{1}H NMR for (TMP)Rh-$OCH_3(CH_3OH)$ Solutions in Benzene/Methanol. *(a). ^{1}H NMR of the Porphyrin Mesityl o-CH_3 Groups.* ^{1}H NMR spectra for the porphyrin mesityl *o*-CH_3 groups in (TMP)Rh-$OCH_3(CH_3OH)$ (**1**) at a series of concentrations of methanol in benzene are illustrated in Figure 2. Rhodium(III) binding of methoxide and methanol on opposite porphyrin faces produces chemical inequivalence of the mesityl *o*-CH_3 groups that is observed in the

Received: October 8, 2010
Published: March 23, 2011

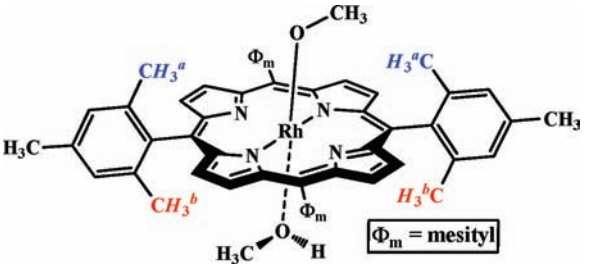

Figure 1. Illustration of the six-coordinate 18-electron species ((TMPRh-OCH$_3$(CH$_3$OH)) (**1**). The mesityl *o*-CH$_3$ groups on opposite faces of the porphyrin are inequivalent.

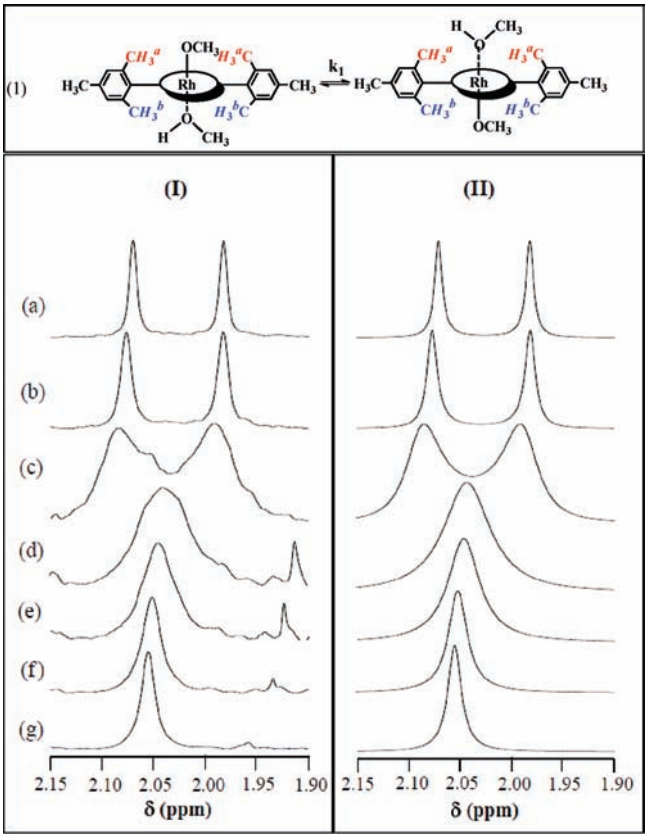

Figure 2. (I) Observed ^{1}H NMR (300 MHz) spectra of porphyrin mesityl *o*-CH$_3$ groups for (TMP)Rh-OCH $_3$(CH$_3$OH) (1.0×10^{-3} M) at 298 K as a function of molar concentration of methanol in C$_6$D$_6$ ([CH $_3$OH]: (a) 0.28 M, (b) 0.35 M, (c) 0.85 M, (d) 1.36 M, (e) 1.73 M, (f) 2.42 M, (g) 4.16 M); (II) gNMR[35] simulated ^{1}H NMR (300 MHz) spectra of porphyrin mesityl *o*-CH $_3$ groups for (TMP)Rh-OCH$_3$(CH$_3$OH) using two-site *o*-CH$_3$ interchange rate constants (a) 3 s^{-1}, (b) 6 s^{-1}, (c) 34 s^{-1}, (d) 132 s^{-1}, (e) 186 s^{-1}, (f) 342 s^{-1}, (g) 540 s^{-1}.

^{1}H NMR (Figure 2, a−c). Merging of the porphyrin mesityl *o*-CH$_3$ resonances into a singlet at concentrations of methanol greater than 1.3 M (Figure 2, d−g) results from dynamic processes which interchange the chemical environments for the two porphyrin faces.

(b). ^{1}H NMR of Coordinated Methoxide and Methanol Groups in ***1***. ^{1}H NMR for (TMP)Rh-OCH$_3$(CH$_3$OH) (**1**) in the high field region ($\delta = -1.5$ ppm to $\delta = -2.5$ ppm) associated with methyl groups for coordinated methoxide and methanol in **1** at a series of methanol concentrations is shown in Figure 3.

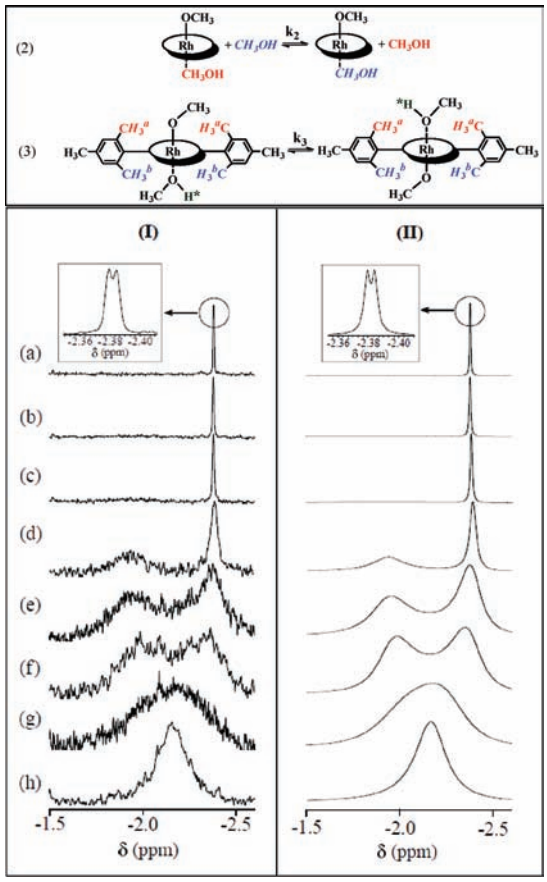

Figure 3. (I) Observed ^{1}H NMR (300 MHz) spectra of (TMP)Rh-OCH$_3$(CH$_3$OH) (1.0×10^{-3} M) in C$_6$D$_6$ showing the high field region for coordinated methanol and methoxide ligands as a function of molar concentration of methanol in C$_6$D$_6$ ([CH$_3$OH]: (a) 0.28 M, (b) 0.35 M, (c) 0.85 M, (d) 1.36 M, (e) 1.73 M, (f) 2.42 M, (g) 4.16 M, (h) 5.25 M); (II) gNMR[35] simulated ^{1}H NMR (300 MHz) spectra for simultaneous proton exchange between coordinated methanol and methoxide ligands and exchange of coordinated methanol with solution using rate constants given in Table 1.

When the methanol concentration is less than 0.3 M, only the high field doublet ($\delta = -2.38$ ppm, $J_{103\ \text{Rh-OCH}}$ = 1.5 Hz) associated with the Rh-OCH$_3$ unit in **1** is observed (Figure 3). Relatively fast exchange of methanol between **1** and the solution results in extreme broadening of the coordinated methanol methyl resonance at concentrations of methanol less than 0.8 M. Exchange of the methanol ligand occurs on one face of the porphyrin and thus does not interchange the mesityl *o*-CH $_3$ groups which is illustrated in Figure 2a. As the methanol concentration in benzene increases from 0.35 M to 1.36 M, a new broad resonance centered at −1.97 ppm appears that narrows as the methanol concentration increases (Figure 3). This resonance is assigned to the coordinated methanol in **1** that is exchanging with methanol in solution. This is an unusual result because increasing the methanol concentration is observed to reduce the rate of methanol exchange into a range where the ^{1}H NMR line width becomes small enough for observation of the methyl resonance for the coordinated methanol in **1**. When the methanol concentration is further increased the ^{1}H NMR resonances at −1.97 ppm and −2.38 ppm pass through a region where they appear as two broadened equally intense peaks that

dx.doi.org/10.1021/ic1020466 |*Inorg. Chem.* 2011, 50, 3313–3319

ultimately merge to an average position (δ = −2.17 ppm) (Figure 3). This observation establishes the assignment of the methanol and methoxide groups in **1** and the presence of dynamic processes that interchange the magnetic environments of the methoxide and methanol ligands on opposite porphyrin faces in (TMP)Rh-$OCH_3(CH_3OH)$.

Additional support for this model is provided by the temperature dependence for the ^{1}H NMR for (TMP)Rh-OCH_3-(CH_3OH) (**1**) (1.0×10^{-3} M) in a 0.10 M methanol solution in deuterated toluene (T = 298−254 K) (Figure 4) . Throughout this range of conditions the methanol ligand exchange from **1** is the only dynamic process that affects the ^{1}H NMR of **1**. At 298 K the methyl resonance for coordinated methanol in **1** is too broad for observation, but the methanol ligand peak appears and narrows as the temperature decreases (281−254 K) (Figure 4).

Table 1. Rate Constants Derived by Simulations in Figures 2 and 3 for Interchange of the Mesityl *o*-Methyl Groups (k_1), Methanol Ligand Exchange (k_2), and Interchange of Porphyrin Faces (k_3) for ((TMP)Rh-$OCH_3(CH_3OH)$) (1.0×10^{-3} M) at a Series of Methanol Molar Concentrations in C_6D_6 (T = 298 K)

$[CH_3OH]$	$\chi_{(CH3OH)}$ [a]	$k_1 = k_3$ [b] (s^{-1})	k_2 [b] (s^{-1})
0.21	0.018	0	900
0.28	0.025	3	880
0.35	0.031	6	640
0.42	0.037	10	340
0.56	0.048	19	200
0.85	0.073	34	150
1.36	0.113	132	95
1.73	0.142	186	25
2.42	0.192	342	50
2.82	0.219	389	63
3.33	0.254	414	90
4.16	0.306	540	125

[a] χ = mole fraction of methanol in C_6D_6. [b] Rate constants for reactions 1−3 (Figures 2, 3).

Interchange of the Porphyrin Face Environments in (TMP)Rh-$OCH_3(CH_3OH)$ (1) Observed by Mesityl *ortho*-Methyl ^{1}H NMR. Inequivalence of the porphyrin faces of (TMP)Rh-$OCH_3(CH_3OH)$ (**1**) results in chemical inequivalence for the porphyrin mesityl *o*-CH_3 groups which is observed in the ^{1}H NMR of **1** (Figure 2). The rate at which the mesityl *o*-CH_3 groups in **1** interchange their chemical environments increases regularly as the concentration of methanol increases (Figure 2). The dynamic process that produces interchange of the environments of the mesityl *o*-CH_3 groups is not the result of direct rotation of the mesityl groups because the barrier for rotation of a porphyrin bonded mesityl group is prohibitively large.[36−40] Hydrogen exchange between the coordinated methanol and the methoxide groups in **1** with methanol in solution is a chemical process that produces an interchange of the environments for the inequivalent porphyrin faces and thus produces mesityl *o*-CH_3 group pseudo rotation . Independent evaluation of the rates for two site *o*-CH_3 exchange provides an indirect measurement for the effective rate constants for interchange of the methoxide and methanol sites on opposite faces of the porphyrin (Figure 2).

The rate constants for interchange between methanol and methoxide sites in **1** for a series of methanol concentrations are obtained indirectly by line shape analysis of the mesityl *o*-CH_3 ^{1}H NMR (Figure 2, Table1). Regular increase in the rate constants for mesityl *o*-CH_3 group pseudo rotation is found to be empirically fitted to a second order dependence on the total methanol molar concentration (Figure 5).

Methanol Ligand Exchange between 1 and Methanol in Solution Observed by ^{1}H NMR. The high field region in the ^{1}H NMR for (TMP)Rh-$OCH_3(CH_3OH)$ (δ = −1.5 ppm to −2.5 ppm) where coordinated methoxide and methanol resonances occur is shown in Figure 3 as a function of methanol concentration. The major changes that occur in the high field ^{1}H NMR region for (TMP)Rh-$OCH_3(CH_3OH)$ as the concentration of CH_3OH increases are the emergence and narrowing of the methyl resonance for a coordinated methanol in **1** (δ = −1.97 ppm) which subsequently merges with the coordinated methoxide (δ = −2.38 ppm) resonance to an averaged shift position (δ = −2.17 ppm) at very high methanol concentration (5.25 M)

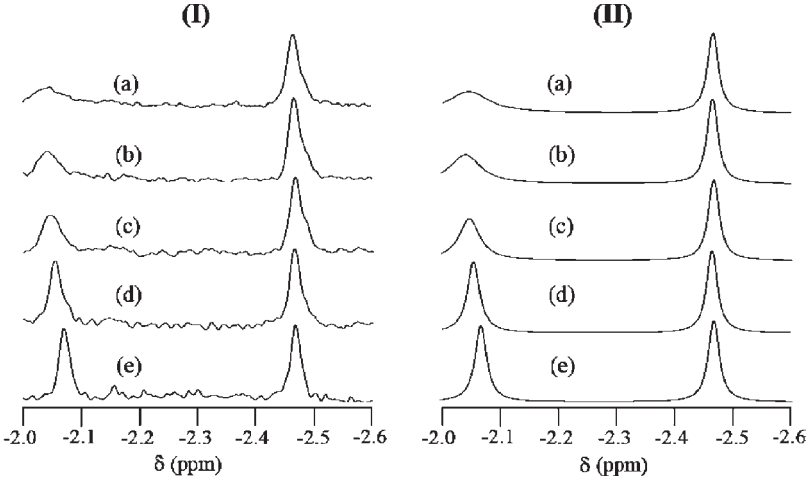

Figure 4. (I) Observed ^{1}H NMR (300 MHz) spectra of (TMP)Rh-$OCH_3(CH_3OH)$ (1.0×10^{-3} M) in $CH_3OH/C_6D_5CD_3$ binary solvent at methanol concentration 0.1 M showing the high field region for coordinated methanol and methoxide ligands as a function of solution temperature (II) gNMR[35] simulated ^{1}H NMR (300 MHz) spectra for exchange of coordinated methanol in **1** with methanol in solution using the rate constants (a) 60 s^{-1} (281 K), (b) 43 s^{-1} (278 K) (c) 22 s^{-1} (275 K) (d) 6 s^{-1} (269 K) (e) 4 s^{-1} (254 K).

dx.doi.org/10.1021/ic1020466 |*Inorg. Chem.* 2011, 50, 3313–3319

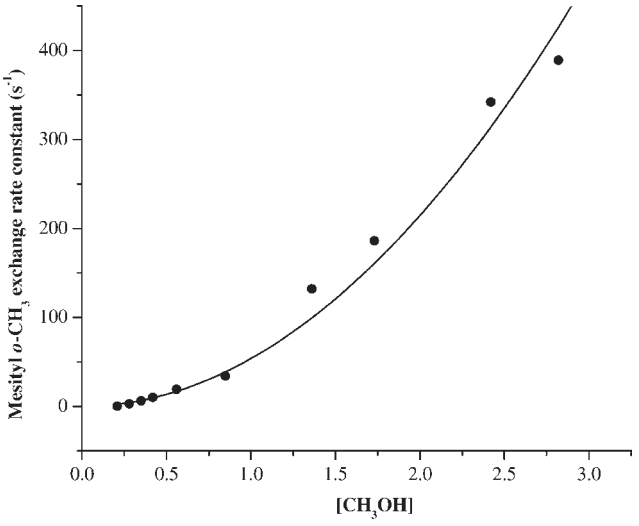

Figure 5. Dependence of the apparent rate constant for porphyrin mesityl *o*-CH_3 pseudorotation of **1** on the total molar concentration of methanol ([CH_3OH]) in methanol−benzene binary solutions. Observed rates of porphyrin mesityl *o*-CH_3 pseudorotation(●). Calculated rate values corresponding to a second order dependence on total molar concentration of methanol (solid line) ($rate_1$ = 53.6 M^{-1} s^{-1} [CH_3OH]^2).

(Figure 3). Changes in the methyl ^{1}H NMR resonances for coordinated methanol and methoxide in **1** are explained in terms of two dynamic processes. Exchange of CH_3OH bonded with rhodium in **1** with the methanol in solution produces selective broadening of the methyl resonance for coordinated methanol, and hydrogen exchange between coordinated methoxide and methanol groups in **1** with methanol in solution results in the merging of the methanol and methoxide resonances in **1** (Figure 3).

Changes in the ^{1}H NMR for coordinated methoxide and methanol in **1** as the concentration of methanol increases are shown in Figure 3, and interpreted in terms of simultaneous methanol ligand and hydrogen exchange processes between **1** and methanol in solution. Independent measurement of the rate constants for interchange of the porphyrin faces by observing the mesityl−ortho methyl pseudo rotation facilitates extracting the rate constants for methanol exchange. Hydrogen exchange between **1** and the methanol solution interchanges the environment of the porphyrin faces, and the exchange of the coordinated methanol with methanol in solution determines the coordinated methanol residence time that selectively influences the coordinated methanol ^{1}H NMR line shape. Setting the rate constants for porphyrin face interchange equal to the rate constant for mesityl *o*-CH_3 interchange aides in evaluation of the rate constant for exchange for coordinated methanol with solution (Table 1) through full line shape analysis using gNMR for the case where both exchange processes are occurring simultaneously (Figure 3, Table 1).

The rate constant for methanol exchange between **1** and the solution at 298 K initially decreases from ∼900 s^{-1} to a minimum of 25 s^{-1} as the methanol concentration increases from 0.20 M to 1.73M, and then increases from 25 s^{-1} to 125 s^{-1} as the methanol concentration further increases from 1.73 to 4.16 M in benzene. The fluctuating ligand exchange kinetic behavior is highly unusual because the rate of an associative ligand interchange increases as the methanol concentration increases, and an ideal dissociative ligand exchange would be independent of the methanol concentration in solution. To our knowledge the observation of fluctuations in a ligand exchange rate with changes in ligand concentration has not been previously reported .

Mechanistic Considerations. *(a). Interchange of the Porphyrin Face Environments in ((TMP)Rh-OCH$_3$(CH$_3$OH)) (**1**) observed by ^{1}H NMR of the Porphyrin Mesityl o-Methyl Groups.* The porphyrin mesityl *o*-CH_3 groups occupy positions on opposing porphyrin faces of (TMP)Rh-OCH $_3$(CH_3OH) (**1**). ^{1}H NMR for the inequivalent *o*-CH_3 groups in **1** provides a probe for the dynamics of processes that interchange the environments of the porphyrin faces. Inequivalence of the porphyrin faces results from methoxide and methanol ligands occupying trans coordination sites in **1**. Proton addition or dissociation from **1** and associative hydrogen interchange of **1** with methanol in solution provide alternate pathways to interchange the environments for the opposing porphyrin faces (Scheme 1). The observed rate of interchange for the methoxide and methanol sites in **1** at 298 K over a wide range of methanol concentrations ([CH_3OH] = 0.21−4.16 M) are relatively well fitted by the square of the total methanol concentration ($rate_1 = k$[CH_3OH] ^{2}) with a second order rate constant of 53.6 M^{-1} s^{-1} (Figure 5).

A second order dependence on the methanol concentration is expected for an associative interchange pathway where there are two methanols in the transition state. If the methanol/benzene solutions were ideal then a second order dependence on the methanol concentration would support an associative interchange pathway (Scheme 1B), but the reported formation of hydrogen bonded clusters of methanol in benzene[33,34] complicates interpretation of the rate dependency on solution composition.

*(b). Methanol Ligand Exchange between **1** and the Methanol/Benzene Solution.* Exchange of methanol between the coordinately and electronically saturated 18-electron complex ((TMP)Rh-OCH$_3$(CH_3OH)) and the solution is expected to be fully dissociative. Activation parameters for the dissociative process will be predominantly determined by thermodynamic and activation parameters for Rh^{III}(CH_3OH) bond dissociation, but there is also a contribution from the activation parameter for the methanol ligand to diffuse away from the metal site and fully enter solution. The rates of dissociative ligand exchange for **1** are expected to be relatively fast because of the small dissociation free energies for methanol from the porphyrin complex **1** and related methanol complex (TMP)Rh-I(CH_3OH) (Supporting Information) which contrasts with the kinetically inert character of fully octahedral d^6 complexes.[41] The rate constant for methanol ligand exchange from **1** in 0.2 M methanol is ∼900 s^{-1} and $\Delta G_1^{\ddagger}$ (298 K) is approximately 13.4 kcal mol^{-1} (k_2(298 K) = 900 s^{-1}; $K^{\ddagger}$ (298 K) = 1.4 × 10^{-10}). The rate constant for methanol ligand exchange from **1** reaches a minimum of 25 s^{-1} at a methanol concentration of 1.7 M ($\chi_{(CH_3OH)}$ = 0.14) which corresponds to a $\Delta G^{\ddagger}$ (289 K) of 15.5 kcal mol^{-1} (k_2 = 25 s^{-1}; $K^{\ddagger}$ (298 K) = 4.2(0.1) × 10^{-12}). A highly unusual feature of this system is that the activation free energy for methanol exchange from **1** is dependent on the solution composition. In ideal solutions the activation free energy for methanol to diffuse away from the metal center and fully enter the solution is the viscosity barrier. In non-ideal binary solutions where one component is a hydrogen bonding associated species the activation energy for diffusion is concentration dependent and larger than the viscosity barrier for either component.[32] The variation in the activation

Scheme 1. Proton Transfer and Associative Interchange for the Methoxide and Methanol Sites in (TMP)Rh-$OCH_3(CH_3OH)$ (1) through Hydrogen Exchange between 1 and Methanol in Solution

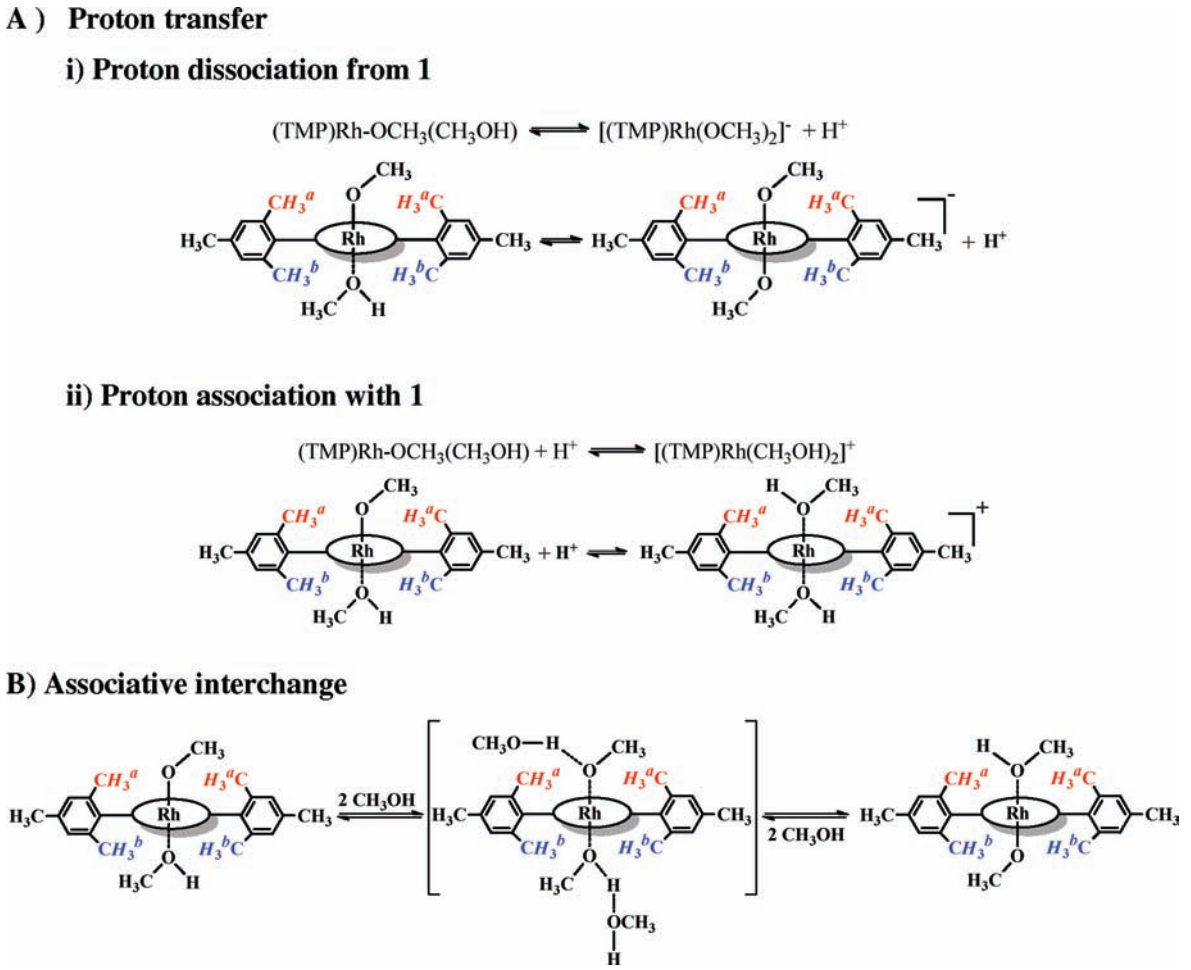

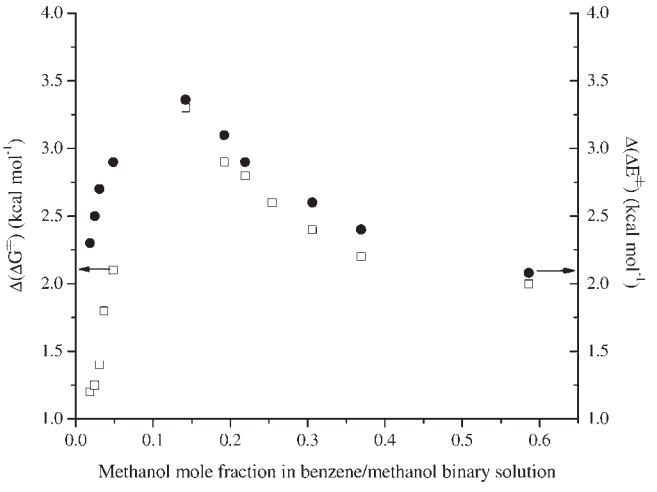

Figure 6. Comparison of the observed change in free energy of activation ($\Delta(\Delta G^{\ddagger})$ for exchange of coordinated methanol in (TMP)Rh-$OCH_3(CH_3OH)$ (**1**) with methanol in bulk (□) and literature values for changes in activation energy for diffusion ($\Delta(\Delta E^{\ddagger})$ (●) of methanol in binary solutions of methanol and benzene (●) as a function of the mole fraction of methanol in benzene.[32]

energy for methanol diffusion in methanol/benzene solutions as a function of the solution composition is shown in Figure 6. Concentration dependence for the change in activation free energy for methanol exchange from **1** has the same general trend, position of maximum and approximately the same magnitude as the concentration dependence of the activation energy for diffusion of methanol in binary methanol and benzene solutions (Figure 6).[32] The unusual fluctuation in the rate constants for methanol ligand exchange from **1** with change in the solution composition is thus tentatively proposed to be caused by the variation in the activation energy for methanol diffusion which is a consequence of the non-ideal behavior of methanol/benzene solutions. This model is based on the total activation free energy for methanol dissociation from **1** consisting of a fixed contribution from the bond breaking process and a variable concentration dependent contribution from the barrier for methanol to diffuse away from the metal and enter into the solution.

SUMMARY

Hydrogen and methanol ligand exchange between (TMP)Rh-$OCH_3(CH_3OH)$ (**1**) and methanol in solution were observed by ^{1}H NMR (Figures 2, 3). Hydrogen exchange for coordinated

dx.doi.org/10.1021/ic1020466 |*Inorg. Chem.* 2011, 50, 3313–3319

methoxide and methanol in **1** with methanol in solution has the effect of interchanging the chemical environments of the porphyrin faces which results in mesityl *o*-CH_3 pseudorotation (Scheme 1). Changes in the ^{1}H NMR for coordinated methoxide and methanol in **1** as the concentration of methanol increases are shown in Figure 3, and interpreted in terms of simultaneous hydrogen and methanol ligand exchange between **1** and methanol in solution. The rate constants for interchange of the porphyrin faces are evaluated by ^{1}H NMR using the mesityl *o*-CH_3 groups. Evaluation of the rate constants for both the methanol ligand exchange and the interchange of the porphyrin face environments is obtained from line shape analysis of the high field methyl resonances for coordinated methoxide and methanol in **1** (Table 1). The rate constants for interchange of the inequivalent porphyrin faces increase regularly with the increase in the mole fraction of methanol, and are approximately fitted by the square of the total methanol concentration (Figure 5). The rates of methanol ligand exchange show an unusual fluctuation as the solution composition changes. Variations in the activation free energy for methanol ligand exchange from **1** correlate with changes in the activation energy for methanol diffusion with solution composition (Figure 6) which occur as a consequence of the non-ideality from hydrogen bonded clusters of methanol in benzene.[32]

EXPERIMENTAL SECTION

General Procedures. All manipulations were performed on a high vacuum line equipped with a Welch Duo-Seal vacuum pump. NMR solvent (C_6D_6) was purchased from Cambridge Isotopes Lab, dried over 4 Å molecular sieves, and degassed by freeze−pump−thaw cycles to remove oxygen. HPLC grade methanol was purchased from Fisher Scientific Company, dried over solid sodium methoxide, and degassed by freeze−pump−thaw cycles to remove oxygen and then vacuum distilled into vacuum adapted Schlenk flasks or NMR tubes. This dry, distilled, oxygen free methanol was used for all the thermodynamic and kinetic studies. All other reagents were purchased from Aldrich Chemicals and used as received.

Proton NMR spectra were obtained on a Bruker-DMX 300, Bruker-AMX360, or a Bruker-AMX500 instrument interfaced to an Aspect 300 computer at ambient temperature. All spectra were referenced against the residual solvent proton peak (benzene-d_6, δ = 7.155 ppm) as the internal standard. Photolysis on rhodium methyl complex [(TMP)Rh-CH_3] to make the metallo radical complex [(TMP)Rh^{II}•] was performed using a Rayonet RPR-100 photochemical reactor.

Tetramesitylporphyrin Rhodium Methoxide Complex ((TMP)Rh-OCH_3) from ((TMP)Rh-I). Rhodium methoxide complex (TMP)Rh-OCH_3 was prepared from the precursor iodide complex (TMP)Rh-I by slightly modifying the published synthetic method developed by Collman and Boulatov.[31] Under dry nitrogen atmosphere, (TMP)Rh-I (5 mg, 4.9×10^{-6} mol) was dissolved in 10 mL of dry CD_2Cl_2. To this solution solid $AgPF_6$ (1.5 mg, 5.9×10^{-6} mol) was added, and the reaction mixture was stirred at room temperature under nitrogen for 2 h. The precipitated AgI was filtered out under inert atmosphere and to the filtrate was added excess solid sodium methoxide ($NaOCH_3$) (0.5 mg, 9.2×10^{-6} mol, approximately 2 equiv), and reaction mixture was stirred under nitrogen for an additional 30 min. The reaction mixture was filtered to remove any solid precipitate, and solvent was removed under vacuum. The solid residue was quickly extracted with benzene under inert atmosphere, and solvent removed under vacuum to yield (TMP)Rh-OCH_3. ^{1}H NMR (CD_2Cl_2) δ(ppm): 8.87 (s, 8H, pyrrole), 7.26 (s, 8H, *m*-phenyl), 2.67 (s, 12H, *p*-CH_3), 2.06 (s, 12H, *o*-CH_3), 1.96 (s, 12H, *o*-CH_3), −2.35 (s, 3H, -OCH_3).

Determination of Rate Constants of Simultaneous Degenerate Proton Exchange between Coordinate Methoxide and Methanol and Exchange of Coordinated Methanol of (TMP)Rh-OCH_3(CH_3OH) with Bulk in Methanol/Benzene (C_6D_6) Mixed Solvent System. To a 300 μL solution of (TMP)Rh-OCH_3 ([(TMP)Rh-OCH_3] ~ 1.0×10^{-3} M) in C_6D_6, methanol (CH_3OH) was added in steps of 2 μL, and the ^{1}H NMR spectrum of the solution was recorded immediately after each addition. Concentration of methanol and (TMP)Rh-OCH_3(CH_3OH) was calculated after each addition taking into consideration the total volume of the sample solution and the initial concentration of (TMP)Rh-OCH_3 present in the solution. The procedure was repeated until the methanol concentration in the sample solution reached a maximum value of 13.3 M.

Full line shape analysis and computational simulation of the resonances for the mesityl *o*-CH_3 groups and coordinated methoxide and methanol resonances of (TMP)Rh-OCH_3(CH_3OH) were performed for each spectrum using gNMR[35] software suite (version 5.0.5.0) and used to evaluate the rate constants for both porphyrin face interchange and exchange of coordinated methanol with methanol in bulk solution that occur simultaneously .

To simulate line shapes of the three regions of interest in the NMR spectra of (TMP)Rh-OCH_3(CH_3OH), by the ^{1}H NMR resonances for the mesityl *o*-CH_3 groups of porphyrin ligand, the metal coordinated methoxide and methanol groups, three different molecules were defined in the gNMR program to simulate the (CH_3O-Rh-(CH_3OH)) fragment of (TMP)Rh-OCH_3(CH_3OH), the mesityl *o*-CH_3 groups on two faces of the tetramesityl porphyrin ligand, and bulk methanol in solution. Detailed definitions of these molecules are given in Supporting Information. The chemical shift, line width, and coupling constant parameters assigned to respective molecules defined in the gNMR platform to initiate simulation of simultaneous hydrogen exchange between coordinated methoxide and methanol groups of (TMP)Rh-OCH_3(CH_3OH) and methanol ligand exchange between (TMP)Rh-OCH_3(CH_3OH) and methanol in solution are actual experimental values obtained directly from the ^{1}H NMR of pure (TMP)Rh-OCH_3, and pure methanol in C_6D_6 without any dynamic exchange process going on in the solutions (Supporting Information).

Three independent dynamic exchange processes accounting for (a) proton exchange between coordinated methnol and methoxide ligands of (TMP)Rh-OCH_3(CH_3OH), (b) exchange of coordinated methanol with methanol in solution, and (c) interchange of nonequivalent porphyrin faces leading to pseudo−rotation of mesityl *o*-CH_3 groups of (TMP) ligand were defined using the three previously defined molecular systems maintaining the molar ratio of each component to be exactly the same as that in each experimental solution of (TMP)Rh-OCH_3(CH_3OH) in methanol/benzene mixed solvent systems. Simulated proton NMR spectra were generated in gNMR by independently varying the rates of the three predefined exchange processes so as to match the line shapes and line widths of the simulations with actual experimental ^{1}H NMR spectra of solutions of (TMP)Rh-OCH_3(CH_3OH) in methanol/benzene mixed solvent medium with gradually increasing molar concentrations of methanol. Thus, the methanol concentration dependent rates for each dynamic process at a particular concentration of methanol in methanol/benzene binary solvent system was determined using gNMR simulation for the range of bulk methanol concentration starting from 0.21 to 13.3 M.

ASSOCIATED CONTENT

Supporting Information. Further details are given in Figures SI 1 to SI 4. This material is available free of charge via the Internet at http://pubs.acs.org.

AUTHOR INFORMATION

Corresponding Author
*E-mail: bwayland@temple.edu.

ACKNOWLEDGMENT

This research was supported by the Department of Energy, Office of Basic Energy Science, through Grant DE-FG02-09ER16000.

REFERENCES

(1) Helfer, D. S.; Phaho, D. S.; Atwood, J. D. *Organometallics* **2006**, *25*, 410–415.
(2) Pyadun, R.; Sukumaran, D.; Bogadi, R.; Atwood, J. D. *J. Am. Chem. Soc.* **2004**, *126*, 12414–12420.
(3) Stahl, S. S.; Labinger, J. A.; Bercaw, J. E. *Angew. Chem., Int. Ed.* **1998**, *37*, 2180–2192.
(4) Stahl, S. S.; Labinger, J. A.; Bercaw, J. E. *J. Am. Chem. Soc.* **1996**, *118*, 5961–5976.
(5) Hong, S. H.; Grubbs, R. H. *J. Am. Chem. Soc.* **2006**, *128*, 3508–3509.
(6) Demirhan, F.; Cagaty, B.; Demir, D.; Baya, M.; Daran, J. C.; Poli, R. *Eur. J. Inorg. Chem.* **2006**, *4*, 757–764.
(7) Demirhan, F.; Taban, G.; Baya, M.; Dioni, C.; Daran, J. C.; Poli, R. *J. Organomet. Chem.* **2006**, *691*, 648–654.
(8) Joo, F.; Kovacs, J.; Benyin, A. C.; Katho, A. *Angew. Chem., Int. Ed.* **1998**, *37*, 969–970.
(9) Breno, K. L.; Ahmed, T. J.; Pluth, M. D.; Blazarek, C.; Tyler, D. R. *Coord. Chem. Rev.* **2006**, *250*, 1141–1151.
(10) Zhang, L.; Fung, C. W.; Chan, K. S. *Organometallics* **2006**, *25*, 5381–5389.
(11) Dorta, R.; Rozenberg, H.; Shimon, L. J. W.; Milstein, D. *Chem.—Eur. J.* **2003**, *9*, 5237–5249.
(12) Blum, O.; Milstein, D. *Angew. Chem., Int. Ed. Engl.* **1995**, *34*, 229–231.
(13) Sponsler, M. B.; Weiller, B. H.; Stoutland, P. O.; Bergman, R. G. *J. Am. Chem. Soc.* **1989**, *111*, 6841–6843.
(14) Monaghan, P. K.; Puddephatt, R. J. *Inorg. Chim. Acta* **1982**, *65*, L59–L61.
(15) Milstein, D. *J. Am. Chem. Soc.* **1986**, *108*, 3525–3526.
(16) Li, S.; Sarkar, S.; Wayland, B. B. *Inorg. Chem.* **2009**, *48*, 8550–8558.
(17) Li, S.; Cui, W.; Wayland, B. B. *Chem. Commun.* **2007**, 4024–4025.
(18) Zhang, J.; Li, S.; Fu, X.; Wayland, B. B. *Dalton Trans.* **2009**, 3661–3663.
(19) Fu, X.; Li, S.; Wayland, B. B. *Inorg. Chem.* **2006**, *45*, 9884–9889.
(20) Fu, X.; Li, S.; Wayland, B. B. *J. Am. Chem. Soc.* **2006**, *128*, 8947–8954.
(21) Fu, X.; Li, S.; Wayland, B. B. *J. Am. Chem. Soc.* **2005**, *127*, 16460–16467.
(22) Fu, X.; Wayland, B. B. *J. Am. Chem. Soc.* **2004**, *126*, 2623–2631.
(23) Joyuban, A.; Soltanpour, S. *J. Chem. Eng. Data* **2010**, *55*, 2951–2963.
(24) Chmielewska, A.; Zurada, M.; Klimaszewski, K.; Bald, A. *J. Chem. Eng. Data* **2009**, *54*, 801–806.
(25) Park, J. H.; Jang, M. D.; Kim, D. S. *J. Chromatogr.* **1990**, *513*, 107–116.
(26) Persson, I. *Pure Appl. Chem.* **1986**, *58*, 1153–1161.
(27) Mandal, S.; Pangarkar, V. G. *J. Membrane Sci.* **2002**, *201*, 175–190.
(28) Kumeev, R. S.; Nikiforov, M. Y.; Totchasov, E. D.; Al'per, G. A. *J. Struct. Chem.* **2008**, *49*, 1120–1123.
(29) Wendt, M. A.; Miller, J.; Weinhold, F.; Farrara, T. C. *Mol. Phys.* **1998**, *93*, 145–151.
(30) Sarkar, S.; Li, S.; Wayland, B. B. *J. Am. Chem. Soc.* **2010**, *132*, 13569–13571.
(31) Collman, J. P.; Boulatov, R. *Inorg. Chem.* **2001**, *40*, 560–563.
(32) McKeigue, K.; Gulari, E. *J. Phys. Chem.* **1984**, *88*, 3472–3479.
(33) Asahi, N.; Nakamura, Y. *J. Mol. Liq.* **2001**, *90*, 85–93.
(34) (a) Adachi, Y.; Nakanishi, K. *Mol. Simul.* **1991**, *6*, 299–310. (b) Jalilian, M. R.; Tayyari, S. F. *Spectrochim. Acta, Part A* **2009**, *73A*, 828–832.
(35) (a) *gNMR*, version 5.0.5.0; Ivory Software, 2005. (b) Rummey, J. M.; Boyce, M. C. *J. Chem. Educ.* **2004**, *81*, 762–763.
(36) Medforth, C. J.; Haddad, R. E.; Muzzi, C. M.; Dooley, N. R.; Jaquinod, L.; Shyr, D. C.; Nurco, D. J.; Olmstead, M. M.; Smith, K. M.; Ma, J.-G.; Shelnutt, J. A. *Inorg. Chem.* **2003**, *42*, 2227–2241.
(37) Eaton, S. S.; Eaton, G. R. *J. Am. Chem. Soc.* **1975**, *97*, 3660–3666.
(38) Eaton, S. S.; Eaton, G. R. *J. Am. Chem. Soc.* **1977**, *99*, 6594–6599.
(39) Eaton, S. S.; Fishwild, D. M.; Eaton, G. R. *Inorg. Chem.* **1978**, *17*, 1542–1545.
(40) Rush, T. S., III; Kozlowski, P. M.; Piffat, C. A.; Kumble, R.; Zgierski, M. Z.; Spiro, T. G. *J. Phys. Chem. B* **2000**, *104*, 5020–5034.
(41) Atwood, J. D. *Inorganic and Organometallic Reaction Mechanisms*, 2nd ed.; Wiley-VCH: Weinheim, Germany, 1997.